Journal of Electrical Engineering & Technology Vol. 6, No. 4, pp. 459~465, 2011 **459**
DOI: 10.5370/JEET.2011.6.4.459

Phasor Estimation Algorithm Based on the Least Square Technique during CT Saturation

Dong-Gyu Lee*, Sang-Hee Kang† and Soon-Ryul Nam*

Abstract – A phasor estimation algorithm based on the least square curve fitting technique for the distorted secondary current due to current transformer (CT) saturation is proposed. The mathematical form of the secondary current during CT saturation is represented as the scaled primary current with magnetizing current. The information on the scaled primary current is estimated using the least square technique, with the measured secondary current in the saturated section. The proposed method can estimate the phasor of a fundamental frequency component during the saturated period. The performance of the algorithm is validated under various fault and CT conditions using a C400 CT model. A series of performance evaluations shows that the proposed phasor estimation algorithm can estimate the phasor of the fundamental frequency component with high accuracy, regardless of fault conditions and CT characteristics.

Keywords: CT saturation, Phasor estimation, Least square fitting

1. Introduction

The current flowing through a power line is measured by a current transformer (CT). As CT is a kind of transformer, the saturation of the magnetic flux in the core may occur when a large primary current flows, which distorts the secondary current of a CT and causes problems in power systems.

Several interesting results on the compensation of secondary current distortion have been published. One stream on this topic is based on the CT model [1]-[4]. Although these algorithms are valid under various fault conditions, they still require the magnetization curve or hysteresis curve based on the given CT parameters.

The other approach is based on the regression technique [5]-[8]. The regression method in [5] detects the saturation using discrete wavelet transform and compensates the distorted section of a secondary current with features extracted from the healthy section using a least square fitting method. The suggested algorithm in [6] only uses a least mean square fitting method without a saturation detection technique. A hybrid phasor estimation method in [7] utilizes partial sum-based and least square-based methods before and after CT saturation. This method can deal with the effect of DC offset and CT saturation. However, these methods require the data after the first saturation is finished; this drawback may result in the delayed operation of protection relays. In [8], a method employing the morphological lifting scheme based on morphological wavelets is used to detect CT saturation. A slope of the magnetizing curve, which is regarded as a straight line in the saturated section, is then calculated to estimate and compensate the magnetizing current of the CT. This method can estimate the scaled down and unsaturated primary current in real time. However, the slope of the magnetizing curve is determined by only a few samples at the start of saturation. The accuracy of this method highly depends on the estimated value of the slope.

In this paper, a phasor estimation algorithm based on the least square fitting technique for the distorted secondary current due to CT saturation is proposed. The mathematical form of the secondary current during CT saturation is represented as the scaled primary current with magnetizing current. The information on the scaled primary current is estimated using the least square technique, with the measured secondary current in the saturated section. The proposed method can estimate the phasor of a fundamental frequency component during the saturated period. The performance of the algorithm is validated under various fault and CT conditions using a C400 CT model. To detect the start and end of saturation in real-time, the algorithm based on the third difference function in [9] is used. A series of performance evaluations shows that the proposed phasor estimation algorithm can estimate the phasor of the fundamental frequency component with high accuracy, regardless of fault conditions and CT characteristics.

† Corresponding Author: Department of Electrical Engineering, Myongji University, Yongin, 449-728, Korea. (shkang@mju.ac.kr)
* Department of Electrical Engineering, Myongji University, Yongin, 449-728, Korea. (d.g.lee@me.com, ptsouth@mju.ac.kr)
Received: November 29, 2010; Accepted: April 5, 2011

2. Phasor Estimation Algorithm

2.1 Basic CT theory

Fig. 1 shows a simplified equivalent circuit of a CT, where L_m is the magnetization inductance, R is the total secondary resistance, i_1 is the primary current referred to the secondary, i_m is the magnetizing current and i_2 is the secondary current.

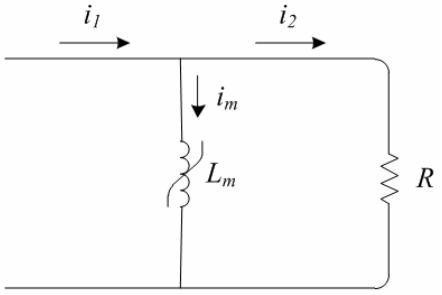

Fig. 1. Simplified equivalent circuit of a CT

The relationship between $i_1(t)$, $i_m(t)$ and $i_2(t)$ is

$$i_2(t) = i_1(t) - i_m(t) \tag{1}$$

The core flux $\varphi(t)$ is related to $i_2(t)$ by the expression

$$N_2 \frac{d\phi(t)}{dt} = Ri_2(t) \tag{2}$$

where N_2 is the number of turns in the secondary winding. Integrating (2) from t_0 to t yields

$$N_2\left(\phi(t) - \phi(t_0)\right) = R\int_{t_0}^{t} i_2(t)dt \tag{3}$$

The core flux $\varphi(t)$ is determined by the magnetization current $i_m(t)$ according to the magnetizing curve.

To simplify, the magnetizing curve in the saturated section is considered a straight line with a slope L_m, as shown in Fig. 2. Hence, (3) can be rewritten as

$$L_m\left(i_m(t) - i_m(t_0)\right) = R\int_{t_0}^{t} i_2(t)dt \tag{4}$$

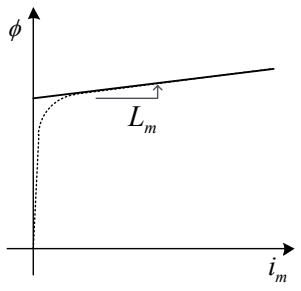

Fig. 2. Magnetization curve of a CT

As the value of $i_m(t_0)$ is near to zero before saturation, (4) can be rewritten as

$$i_m(t) = \frac{R}{L_m}\int_{t_0}^{t} i_2(t)dt \tag{5}$$

2.2 Phasor estimation during CT saturation

The fault current flowing through a primary circuit can be generally considered as the combination of an exponentially decaying DC offset and sinusoidal components. Thus $i_1(t)$ can be expressed as

$$i_1(t) = \mathrm{A}_0 e^{-t/\tau} + \sum_{k=1}^{M} \mathrm{A}_k \sin(kw_0 t + \varphi_k) \tag{6}$$

where τ and A_0 are the time constant and the magnitude of a DC offset component, A_k and φ_k are the amplitude and the phase angle of the k^{th} harmonic component, and M is the highest order of harmonic component present in the signal.

By substituting (5) and (6) into (1) and rearranging at time $t = t_1$, the secondary current $i_2(t)$ during the CT saturation period can be rewritten as

$$\begin{aligned} i_2(t_1) = {} & \mathrm{A}_0 e^{-t_1/\tau} + \sum_{k=1}^{M} \mathrm{A}_k \sin(kw_0 t_1 + \varphi_k) \\ & - \frac{R}{L_m}\int_{t_0}^{t_1} i_2(t)dt \end{aligned} \tag{7}$$

Expanding $e^{-t_1/\tau}$ using the Taylor series is possible as follows:

$$e^{-\Delta t/\tau} = 1 - \frac{\Delta t}{\tau} + \frac{1}{2!}\left(\frac{\Delta t}{\tau}\right)^2 - \frac{1}{3!}\left(\frac{\Delta t}{\tau}\right)^3 + \cdots \tag{8}$$

where Δt is the sampling interval.

The numerical approximation of the integral of the secondary current in (7) can be implemented using a trapezoidal method as follows:

$$\int_{t}^{t+\Delta t} i_2(t)dt = \frac{\Delta t}{2}\left(i_2(t) + i_2(t+\Delta t)\right) \tag{9}$$

Higher-order harmonics can be blocked by the signal conditioning equipment such as an analog low-pass filter. Thus, assuming that the harmonic components higher than the fifth order are effectively blocked by a low-pass filter, and that the even harmonics are hardly present in the power system signals, (7) can be represented as

$$\begin{aligned} i_2(t_1) = {} & a_{11}x_1 + a_{21}x_2 + a_{31}x_3 + a_{41}x_4 + a_{51}x_5 \\ & + a_{61}x_6 + a_{71}x_7 + a_{81}x_8 + a_{91}x_9 + a_{101}x_{10} \end{aligned} \tag{10}$$

where

$$x_1 = A_0 \ , \ x_2 = -A_0(1/\tau) \ , \ x_3 = A_0(1/\tau)$$
$$x_4 = A_1 \cos\varphi_1 \ , \ x_5 = A_1 \sin\varphi_1 \ , \ x_6 = R/L_m$$
$$x_7 = A_3 \cos\varphi_3 \ , \ x_8 = A_3 \sin\varphi_3$$
$$x_9 = A_5 \sin\varphi_5 \quad x_{10} = A_5 \sin\varphi_5$$
$$a_{11} = 1 \ , \ a_{21} = t_1 \ , \ a_{31} = t_1^2/2$$
$$a_{41} = \sin(w_0 t_1) \ , \quad a_{51} = \cos(w_0 t_1) \ , \quad a_{61} = \int_{t_0}^{t_1} i_2(t)dt$$
$$a_{71} = \sin(3w_0 t_1) \ , \ a_{81} = \cos(3w_0 t_1)$$
$$a_{91} = \sin(5w_0 t_1) \ , \ a_{101} = \cos(5w_0 t_1)$$

If the current is sampled with a specific time interval, Δt, (10) can be expanded with each current sample to the necessary extent. The equations can be written in the matrix forms as follows:

$$\underset{m\times 1}{\mathbf{I}} = \underset{m\times 10}{\mathbf{A}} \cdot \underset{10\times 1}{\mathbf{X}} \tag{11}$$

The elements of matrix **A** depend on the time reference and the sampling interval, which can be predetermined in an off-line mode. Matrix **I** made up of the sampled current data during the CT saturation period is also known. If the number of current samples, m, is greater than the number of unknown variables, matrix **X** composed of the unknown variables can be determined using the least square technique as follows:

$$\mathbf{X} = \left[\mathbf{A}^T \cdot \mathbf{A}\right]^{-1} \cdot \mathbf{A}^T \cdot \mathbf{I} \tag{12}$$

Finally, the phasor of the fundamental frequency component at time t_1 can be obtained as (13)

$$x_4(t_1) + jx_5(t_1) = A_1 \cos\varphi_1 + jA_1 \sin\varphi_1 \tag{13}$$

After the first saturation is completed, the phasor can be estimated using any method suggested in [5]-[7]. Until then, the phasor is given by

$$x_4(t_1 + p\Delta t) + jx_5(t_1 + p\Delta t) = \left(x_4(t_1) + jx_5(t_1)\right)e^{-j2\pi p/N} \tag{14}$$

where N is the number of samples per cycle.

3. Performance Evaluation

3.1 System configuration

The performance of the proposed algorithm is evaluated for various faults on a 345 kV, 100 km simple overhead transmission line, as shown in Fig. 3.

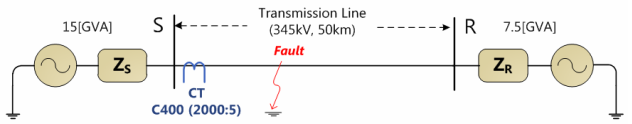

Fig. 3. Single line diagram of the model system

The simulated fault cases are single phase-to-ground faults located 2 km from the S bus. The CT modeling described in [10] is used to simulate the remanent flux and a resistive burden of 4.03 Ω is connected to a C400 CT (2000:5). The saturation point of (2.047 A, 1.512 Vs) is selected to generate hysteresis data using HYSDAT, which is an auxiliary program in EMTP.

In the proposed algorithm, the magnetization current is assumed to be zero before saturation. To consider the effect of the assumption, two kinds of hysteresis loops are used, as shown in Fig. 4. The saturation points of the two hysteresis loops are the same, but the hysteresis losses are different. In Case 1, the original hysteresis loop generated by the HYSDAT subroutine is used in the CT modeling, whereas in Case 2, a revised loop is used to increase the magnetization current before saturation.

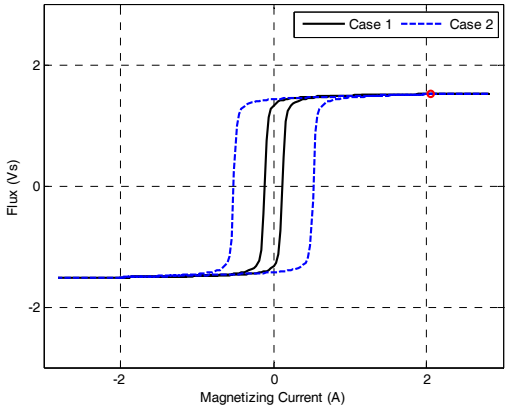

Fig. 4. Hysteresis loops used in the CT modeling

The sampling frequency is set to 3,840 Hz, *i.e.*, 64 samples per cycle in 60 Hz systems. The number of current samples, m, for the least square fitting is set to 20. The current signal is preprocessed by a second-order Butterworth low-pass filter with the gain of 0.1 at the stop-band cutoff frequency of 1,920 Hz to remove the harmonics and prevent aliasing errors. To detect the start and end of saturation in real-time, the algorithm based on the third difference function in [9] is used.

3.2 Case studies

Figs. 5 and 6 show the test results of the proposed algorithm for Case 1. To demonstrate the accuracy of the

proposed algorithm, the estimated results using the scaled primary current are also shown in each figure.

Figs. 5(a) and 6(a) show the scaled primary current referred to the secondary side and the measured secondary current. Figs. 5(b) and 6(b) show the actual and estimated magnetizing currents and the detected saturation section by the third difference function. The estimated magnetizing current is calculated using a_{61} and x_6 in (10). In this case, the magnetizing current is close to zero before saturation, as shown in each enlarged figure. Figs. 5(c) and 6(c) show the estimated dc component using (12). Figs. 5(d) and 6(d) show the estimated real and imaginary parts of the fundamental frequency component using (12). Even if the estimated dc component contains some errors, the estimated real and imaginary parts of the fundamental frequency component are still nearly equal to the results estimated using the primary current. Figs. 5(e) and 6(e) show the real and imaginary parts of the estimated phasor using (13).

The error of the estimated dc component can come from the magnetization curve as a straight line with a slope. However, the magnetization curve is not a straight line around the saturation point. Although this assumption may lead to some difference between the input signal and the mathematical form in (7), the difference exponentially decreases as the magnetizing current increases. Therefore, the difference only affects the estimated magnetizing current and the dc component. Moreover, the more the CT is severely saturated, the more the magnetization curve is close to a straight line. This explains why the estimated magnetizing current and the dc component by the proposed algorithm are more correct when the CT is severely saturated.

Figs. 7 and 8 show the test results of the proposed

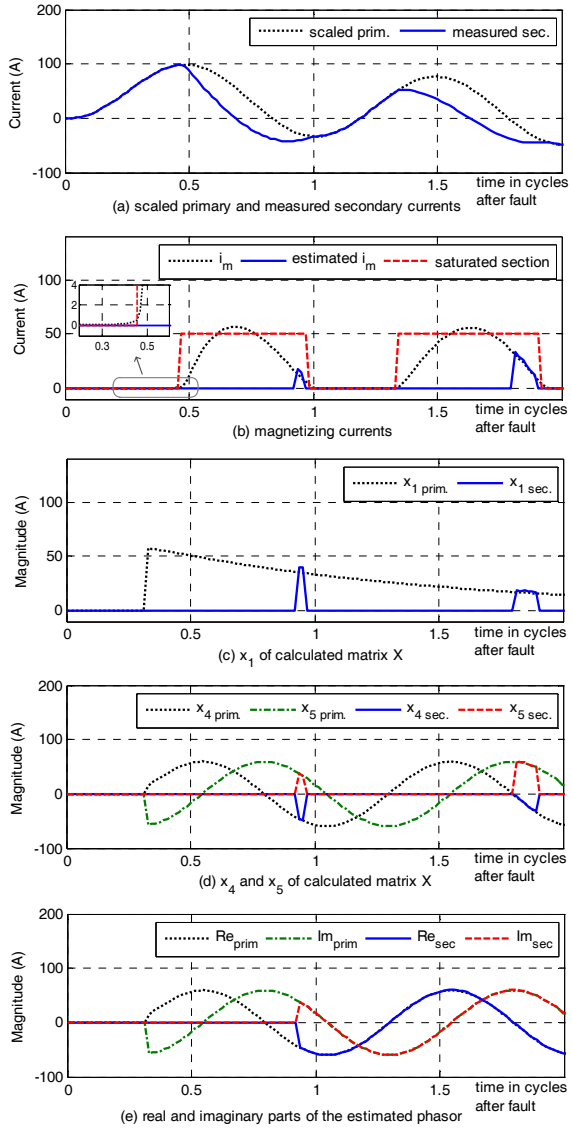

Fig. 5. Test results for Case 1 (Fault inception angle 0°, Remanent flux 0%)

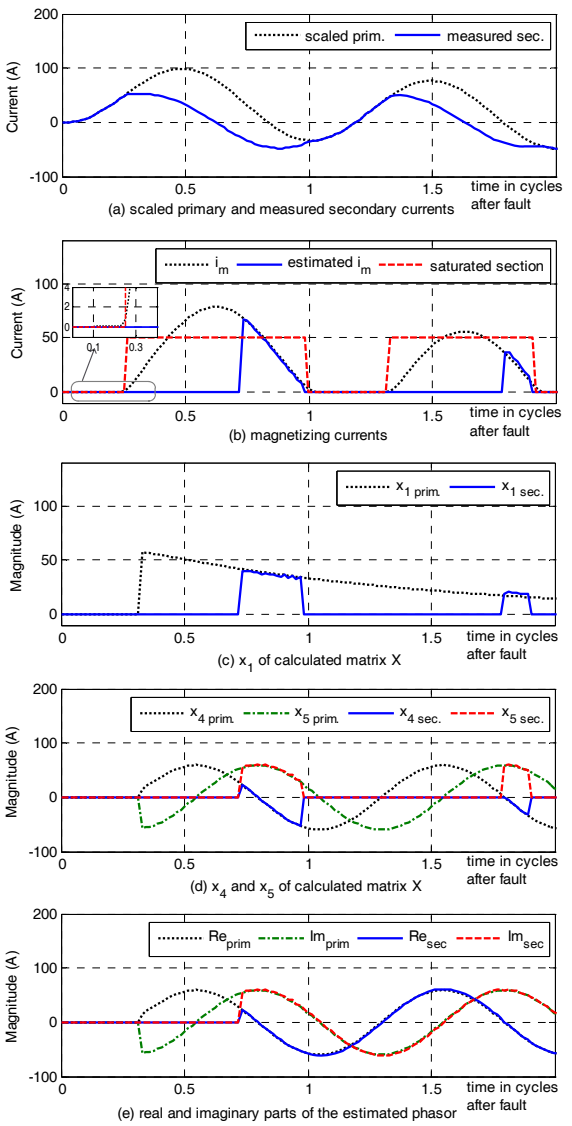

Fig. 6. Test results for Case 1 (Fault inception angle 0°, Remanent flux 80%)

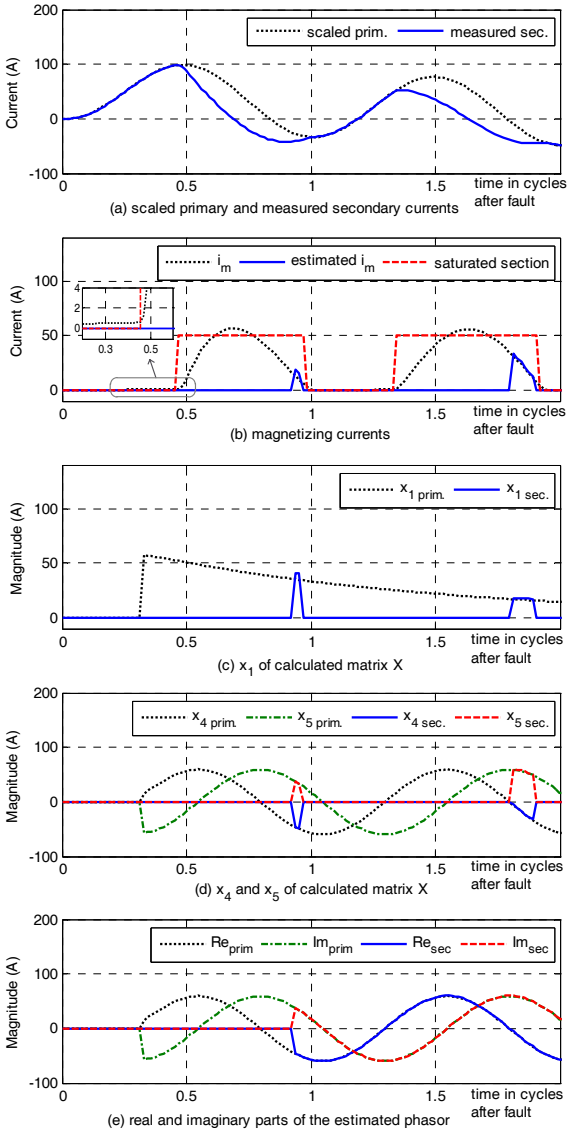

Fig. 7. Test results for Case 2 (Fault inception angle 0°, Remanent flux 0%)

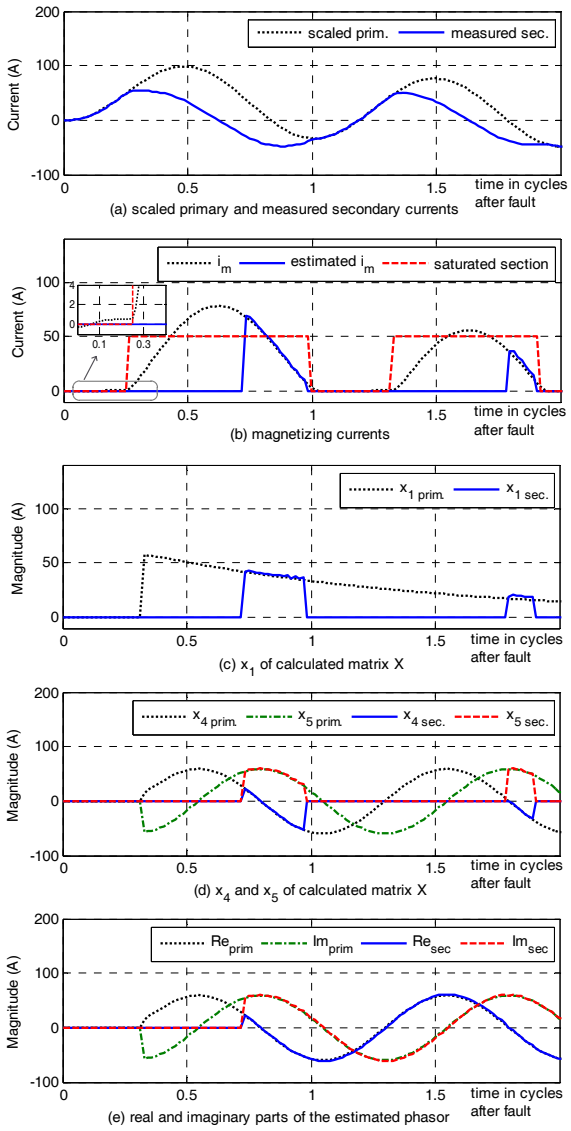

Fig. 8. Test results for Case 2 (Fault inception angle 0°, Remanent flux 80%)

algorithm for Case 2. In this case, the magnetizing current before saturation is greater than that in Case 1, as shown in the enlarged inner figures in Fig. (b). However, the magnetizing current term ignored in (4) is a constant value, thus its frequency response may belong to the dc component. As a result, the estimated dc component and the magnetizing current are slightly different from those in Case 1. However, the real and imaginary parts of the estimated phasor are nearly the same with the results of Case 1.

Based on these results, it is clear that the proposed algorithm can estimate the accurate phasor of the fundamental frequency component before the CT leaves the saturation period. Moreover, the proposed algorithm can quickly estimate the phasor when the CT is deeply saturated.

Fig. 9 shows the time responses of the proposed algorithm and the least square (LS)-based algorithm in [6] for the 0° fault with 80% remanent flux. The LS-based algorithm uses the samples obtained from not only the first unsaturated waveform portion but also the second unsaturated waveform portion. However, the proposed algorithm only uses the first saturated waveform portion, which explains why the proposed algorithm can estimate the accurate phasor faster than the LS-based algorithm.

4. Conclusion

A phasor estimation algorithm based on the least square curve fitting technique for the distorted secondary current due to CT saturation was described. The mathematical form of the secondary current during CT saturation was represented as the scaled primary current with the

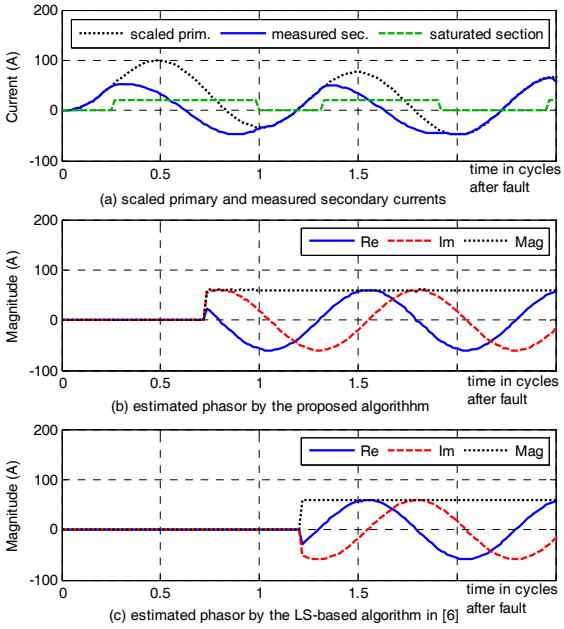

Fig. 9. Time response comparison in Case 1 (Fault inception angle 0°, Remanent flux 80%)

magnetizing current. The information on the scaled primary current was estimated using the least square technique with the measured secondary current in the saturated section. Then, the proposed method can estimated the phasor of the fundamental frequency component of a current signal, especially during the saturated period.

The performance of the algorithm was validated under various fault and CT conditions using a C400 CT model. A series of performance evaluations showed that the proposed phasor estimation algorithm can estimate the phasor of the fundamental frequency component with high accuracy, regardless of fault conditions and CT characteristics.

The proposed algorithm is more effective when a CT is deeply saturated with a large remanent flux in the CT core. Therefore, the proposed algorithm is considered a useful method for the phasor estimation of the fault current signals in power system applications. For example, it can decrease the unnecessary time delay of the protection relays.

Acknowledgements

This work was supported by the National Research Foundation of Korea (NRF) grant funded by the Korea government (MEST) (No. 2011-0000151) and the 2nd Brain Korea 21 Project.

References

[1] Y. C. Kang, J. K. Park, S. H. Kang, A. T. Johns and R. K. Aggarwal, "An Algorithm for Compensating the Secondary Current of Current Transformers", *IEEE Trans. Power Delivery*, vol. 12, no. 1, pp.116-124, Jan. 1997

[2] N. Locci and C. Muscas, "A Digital Compensation Method for Improving Current Transformer Accuracy", *IEEE Trans. Power Delivery*, vol. 15, no. 4, pp. 1104–1109, Oct. 2000

[3] N. Locci and C. Muscas, "Hysteresis and Eddy Current Compensation in Current Transformer", *IEEE Trans. Power Delivery*, vol. 16, no. 2, pp.154-159, April 2001

[4] Y. C. Kang, U. J. Lim, S.H. Kang and P.A. Crossley, "Compensation of the Distortion in the Secondary Current Caused by Saturation and Remanence in a CT", *IEEE Trans. Power Delivery*, vol. 19, no. 4, Oct. 2004.

[5] F. Li, Y. Li and R. K. Aggarwal, "Combined Wavelet Transform and Regression Technique for Secondary Current Compensation of Current Transformers", *IEE Proc. Generation, Transmission and Distribution*, vol. 149, no. 4, pp.497-503, July 2002.

[6] J. Pan, K. Vu and Y. Hu, "An Efficient Compensation Algorithm for Current Transformer Saturation Effects", *IEEE Trans. Power Delivery*, vol. 19, no. 4, pp. 1623–1628, Oct. 2004.

[7] Soon-Ryul Nam, Jong-Young Park, Sang-Hee Kang and Mladen Kezunovic, "Phasor Estimation in the Presence of DC Offset and CT Saturation", *IEEE Trans. Power Delivery*, vol. 24, no. 4, pp. 1842–1849, Oct. 2009.

[8] Z. Lu, J. S. Smith and Q. H. Wu, "Morphological Lifting Scheme for Current Transformer Saturation Detection and Compensation", *IEEE Trans. Circuits and Systems I: Regular Papers*, vol. 55, no. 10, pp. 3349 - 3357, Nov. 2008

[9] Y. C. Kang, S. H. Ok and S. H. Kang, "A CT Saturation Detection Algorithm", *IEEE Trans. Power Delivery*, vol. 19, no. 1, pp. 78–85, Jan. 2004

[10] M. Kezunovic, Lj. Kojovic, A. Abur, C. W. Fromen, D. R. Sevcik and F. Phillips, "Experimental evaluation of EMTP-based current transformer models for protective relay transient study", *IEEE Trans. Power Delivery*, vol. 9, no. 1, pp. 405-413, Jan. 1994

Dong-Gyu Lee received the B.S., M.S. and Ph.D. degrees in electrical engineering from Myongji University, Korea, in 2002, 2004 and 2010, respectively. His main research interests are power system protection.

Sang-Hee Kang received the B.S., M.S. and Ph.D. degrees from Seoul National University, Korea in 1985, 1987 and 1993, respectively. He was a visiting fellow and a visiting scholar at the University of Bath, UK in 1991 and 1999. He is a professor at Myongji University, Korea. He has been also with Next-generation Power Technology Center, Korea since 2001. He was an honorary academic visitor at the University of Manchester, UK in 2007. His research interest is to develop digital protection systems for power systems using digital signal processing techniques.

Soon-Ryul Nam received the B.S., M.S., and Ph.D. degrees in electrical engineering from Seoul National University, Seoul, Korea in 1996, 1998 and 2002, respectively. He is an associate professor at Myongji University, Yongin, Korea. His research interests are the protection, control, and automation of power systems.